Hindawi Publishing Corporation
Journal of Biomedicine and Biotechnology
Volume 2009, Article ID 875629, 8 pages
doi:10.1155/2009/875629

Research Article

Separation and Purification of Two Flavone Glucuronides from *Erigeron multiradiatus* (Lindl.) Benth with Macroporous Resins

Zhi-feng Zhang,[1] Yuan Liu,[1] Pei Luo,[2] and Hao Zhang[2]

[1] *Ethnic Pharmaceutical Institute, Southwest University for Nationalities, Chengdu 610041, China*
[2] *West China School of Pharmacy, Sichuan University, Chengdu 610041, China*

Correspondence should be addressed to Zhi-feng Zhang, zhangzhf99@gmail.com

Received 21 March 2009; Revised 30 June 2009; Accepted 19 August 2009

Recommended by H. M. Häggman

Scutellarein-7-*O*-*β*-D-glucuronide (SG) and apigenin-7-*O*-*β*-D-glucuronide (AG) are two major bioactive constituents in *Erigeron multiradiatus*. In this study, a simple method for preparative separation of the two flavone glucuronides was established with macroporous resins. The performance and adsorption characteristics of eight macroporous resins including AB-8, HPD100, HPD450, HPD600, D100, D101, D141 and D160 had been evaluated. The results confirmed that D141 resin was preferred choice, which offered the best adsorption and desorption capacities for the two glucuronides among the tested resins. Sorption isotherms were constructed for D141 resin and fitted well to the Freundlich and Langmuir models ($R^2 > 0.95$). After one run treatment with D141 resin, the two constituents' content was increased from 2.14% and 1.34% in the crude extract of *E. multiradiatus* to 24.63% and 18.42% in the final products with the recoveries of 82.5% and 85.4%, respectively. The enrichment of SG and AG can be easily and effectively achieved via adsorption and desorption on D141 resin, and the method can be referenced for large-scale separation and purification of flavone glucuronides from herbal raw materials.

1. Introduction

Erigeron multiradiatus (Lindl.) Benth is an important traditional Tibetan medicine herbs used for thousands of years to treat various diseases, such as hypopepsia, enteronitis diarrhea, hepatitis, adenolymphitis rheumatism, and hemiparalysis [1]. Our previous researches on phytochemistry showed that *E. multiradiatus* contained a notable amount of flavonoids, and scutellarein-7-*O*-*β*-D-glucuronide (SG) and apigenin-7-*O*-*β*-D-glucuronide (AG) are the major flavonoids constituents in *E. multiradiatus* with significant anti-inflammatory activities [2]. Various biological and pharmacological activities have also been attributed to these two components, such as dilating blood vessel, improving microcirculation, increasing cerebral blood flow, and inhibiting platelet aggregation activity [3–6]. Their chemical structures are shown in Figure 1.

The conventional separation method of flavonoids compounds was performed by solid-liquid extraction or liquid-liquid extraction using different solvents and then followed by polyamide chromatography, gel chromatography, silica gel column and ODS, and so forth [7–10]. However, all of them have the same disadvantage such as taking a long time, consuming large amounts of solvent and the low recovery. Macroporous resins, a nontype ion-exchange groups with large pore structure of the polymer adsorbent, is one of the most efficient separation materials. The adsorption properties of macroporous resin were correlated with their surface adsorption, sieve classification, surface electrical property and hydrogen bonding interactions, and so forth [11, 12]. They are durable nonpolar, middle polar, and polar macroporous polymers having a high adsorption capacity, with relative low cost and easy regeneration, and exhibit good performances in recovering and separating of plant secondary metabolites. They have been successfully applied for separation of flavonoids, saponins, and alkaloids

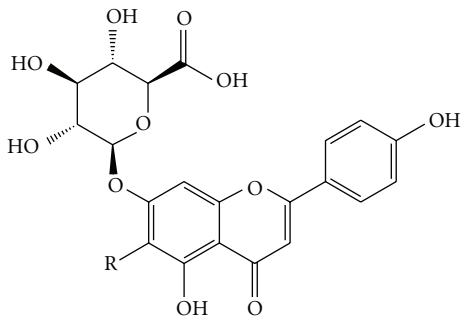

1 R = OH
2 R = H

Figure 1: Chemical Structure of compounds 1 and 2 identified from *E. multiradiatus*. (1) Scutellarein-7-*O*-*β*-glucuronide; (2) Apigenin-7-*O*-*β*-glucuronide.

from traditional Chinese medicine (TCM) or herbs [13–17].

Therefore, the aims of this present study were to investigate the adsorption and desorption properties of SG and AG on different macroporous resins and were designed to develop an effective methods for preparative separation of SG and AG from *E. multiradiatus* with optimal resins. The result in this study is significant for the enrichment and purification of flavone glucuronides from *E. multiradiatus*.

2. Experimental

2.1. Chemicals and Reagents. Methanol of HPLC grade was purchased from Sigma-Aldrich (Steinheim, Germany). All the other reagents were of analytical grade, and deionized water was purified by a Milli-Q water-purification system from Millipore (Bedford, MA, USA). SG and AG were extracted, isolated, and purified from fresh herb of *E. multiradiatus* in our laboratory. The purified compounds were identified by electrospray ionization (ESIs)-MS, ^{1}H NMR, and ^{13}C NMR spectrometric techniques and comparing with literatures, the purities were found to be greater than 97% based on the percentage of total peak area by HPLC analysis.

Appropriate amounts of standards were dissolved in methanol to yield the stock solutions at concentration of 0.54 mg/mL and 0.50 mg/mL for SG and AG, respectively. All solutions were filtered through 0.45 μm membranes (Fisher Scientific) before HPLC.

2.2. Adsorbents. Macroporous resins including AB-8, HPD100, HPD450, HPD600, D100, D101, D141, and D160 were supplied from Cangzhou Bon Chemical Co., Ltd. (Hebei, China) and Chenguang Research Institute of Chemical Industry (Chengdu, China). Their physical properties are summarized in Table 1. The resins were pretreated by soaking in 95% ethanol for 24 hours to remove the monomers and porogenic agents trapped inside the pores during the synthesis process and then washed by deionized water thoroughly. The moisture contents of the tested resins were determined by drying at 70 °C to constant weight in a drying oven. The moisture contents are shown in Table 2.

2.3. Preparation of E. Multiradiatus Extracts Sample Solutions. *E. multiradiatus*, whole plants collected in "luoguoliangzi" Luhuo County, Ganzi Tibetan Autonomous Prefecture, Sichuan Province, China, 2006, was authenticated by Professor Tianzhi Wang in the West China School of Pharmacy, Sichuan University, where a voucher specimen was deposited (number 12025). The material was dried at room temperature, grounded to powder, and then sieved (20 mesh). And this powder (1000 g) was extracted by refluxing with 5000 mL of ethanol-water (40 : 60, v/v) solution for 2 hours, repeated three times. The supernatant clear extract was concentrated to one fifth of the original volume by removing the ethanol solvent in a rotary evaporator (SBW-1, Shanghai Shenko Instrument Co., China) at 50 °C. Distilled water was added to get SG and AG solutions at the concentration of 1.18 mg/mL and 0.81 mg/mL, respectively.

2.4. HPLC Analysis of SG and AG. Quantification of SG and AG was carried out by HPLC on a Shimadzu LC-10Atvp System (Shimadzu Corp., Kyoto, Japan), consisting of LC-10ATvp binary pump, an SPD-M10Avp photodiode array detector (PDA), a CTO-10Asvp column oven, a SCL-10Avp system controller, and an N2000 workstation. Analysis was performed on a C_{18} reversed-phase column (Kromasil, 250 mm × 4.6 mm, 5 μm) (Eka Chemicals AB, Bohus, Sweden). The mobile phase consisted of methanol-0.4% acetic acid (40 : 60, v/v). The flow rate was 1.0 mL·min^{-1} throughout the run and column temperature was maintained at 35 °C. The detection wavelength was set at 335 nm for acquiring chromatograms. The retention time of SG and AG was 16.8 minutes and 27.5 minutes, respectively. The working calibration curve based on scutellarin standard solutions showed good linearity over the range of 0.54–5.4 μg and 0.5–5.0 μg. The regression lines for SG and AG were $y = 7351.4x - 4832.5$ ($r = 0.9999$) and $y = 5947.6x - 8548.9$ ($r = 0.9999$), respectively, where y is the peak area and x is the concentration (mg/mL).

2.5. Static Adsorption and Desorption Tests. The static adsorption tests of *E. multiradiatus* extracts on macroporous resins were performed as follows: preweighed amounts of different hydrated resins (equal to 2 g dry resin) were put into flasks with a lid; 20 mL aqueous solution of SG and AG extracts described above was added. The flasks were sealed tightly and shaken (120 rpm) for 6 hours at 25 °C. After adsorption equilibrium was reached, the supernatant after adsorption was analyzed by HPLC. Then the resin was first washed by deionized water for 4 times and desorbed with 40 mL ethanol-water (80 : 20, v/v) solution. The desorption solutions were also analyzed by HPLC. Candidate resins were selected in terms of their adsorption capacities, desorption capacities, and desorption ratios.

The adsorption kinetics curve of SG and AG in the preliminarily selected resins was also studied according to the above-mentioned method. The concentrations of SG and

Table 1: Physical properties of the macroporous resins used.

Name	Particle diameter (mm)	Surface area (m^2/g)	Average pore diameter (nm)	Polarity
AB-8	0.3–1.25	480–520	130–140	Weak -polar
HPD100	0.3–1.2	650–700	85–90	Nonpolar
HPD450	0.25–0.84	500–550	90–110	Mid-polar
HPD600	0.3–1.2	550–600	75–110	Polar
D100	0.315–0.9	500–600	100–150	Nonpolar
D101	0.25–0.84	500–550	90–100	Nonpolar
D141	0.315–0.9	500–600	80–110	Weak-polar
D160	0.315–0.9	500–600	100–150	Polar

Table 2: Results of the moisture contents of different resins.

Name	Moisture content (%)	Name	Moisture content (%)
AB-8	67.3	D100	67.8
HPD100	70.2	D101	70.5
HPD450	71.3	D141	69.4
HPD600	66.5	D160	72.8

AG in sample solution after adsorption of a certain time were monitored at equal time intervals till equilibration. The adsorption isotherms of SG and AG on the selected D141 resin were also studied by contacting 20 mL sample solutions of *E. multiradiatus* extracts at different concentrations with the preweighed hydrated resins (equal to 2 g dry resin) and shaking for 6 hours at 25 °C. The initial and equilibrium concentrations were determined by HPLC and their degrees of fitness to Freundlich equations were investigated [16, 17].

The adsorption-desorption properties of the selected resins under different conditions including initial concentration and pH of sample solution and concentration of ethanol for desorption were also evaluated.

2.6. Dynamic Adsorption and Desorption Tests. Dynamic adsorption and desorption experiments were carried out in a glass column (1.2 cm × 30 cm) wet-packed with hydrated resins (equal to 5 g dry resin) of the selected resin. The bed volume (BV) of the resin was 20 mL. The flow rate of sample solution was 1.5 BV/h through the glass column. After reaching adsorptive equilibrium, the loading of the sample was stopped. The adsorbate-laden column was washed firstly by deionized water with 4 BV and then desorbed with ethanol-aqueous solution. Each part of desorption solutions was concentrated to dryness under vacuum and weighed to calculate the contents of SG and AG by HPLC analysis. Dynamic adsorption and desorption tests were repeated three times under optimal conditions, and the kinetic adsorption capacity, the purity, and yield of SG and AG were calculated.

2.7. Adsorption and Desorption Capacity and Desorption Ratio. The adsorption and desorption properties of different resins are quantified with the following equations.

Adsorption evaluation:

$$q_e = \frac{(C_0 - C_e)V_i}{W}, \tag{1}$$

where q_e is the adsorption capacity at adsorption equilibrium (mg/g resin); C_0 and C_e are the initial and equilibrium concentrations of solutes in the solutions, respectively (mg/mL); V_i is the volume of the initial sample solution (mL) and W is the weight of the tested dry resins (g).

Desorption evaluation is

$$Q_d = \frac{C_d V_d}{W},$$
$$D = \frac{C_d V_d}{(Co - Ce)V_i} \times 100\%, \tag{2}$$

where Q_d is the desorption capacity after adsorption equilibrium (mg/g dry resin); D is the desorption ratio (%); C_d is the concentration of the solutes in the desorption solutions (mg/mL); V_d is the volume of the desorption solution; Co, Ce, W, and V_i are the same as those defined above.

2.8. Recovery. Recovery was used to evaluate the accuracy of the method. It was determined by calculating the content of SG and AG of the extracts before and after separation on column packed with D141 and described with the following equations:

$$\mathrm{R} = \frac{\text{the content of SG and AG after column}}{\text{the content of SG and AG before column}} \times 100\%. \tag{3}$$

3. Results and Discussion

3.1. Results of Adsorption and Desorption Capacity and Desorption Ratios. Eight macroporous resins with different physical properties were employed for enrichment and purification of SG and AG, and the results were shown in Figures 2 and 3. The adsorption capacity towards SG and AG on HPD100, D101, and D141 resins was considerably higher than those of other resins, which correlates with the capabilities of the resins and the chemical features of the adsorbed substance. The weak-polar resin D141 exhibited the best adsorption and desorption capabilities.

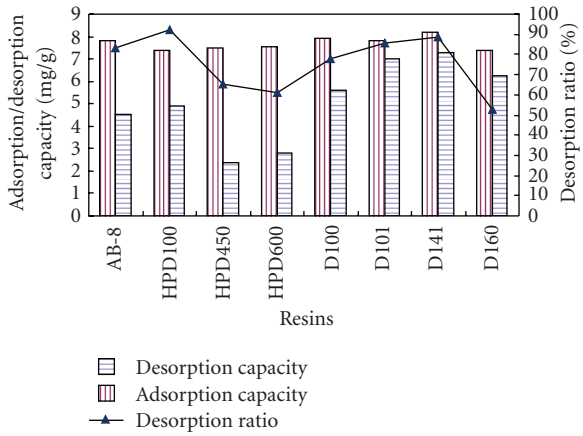

Figure 2: Adsorption capacity, desorption capacity, and desorption ratio of SG on different resins.

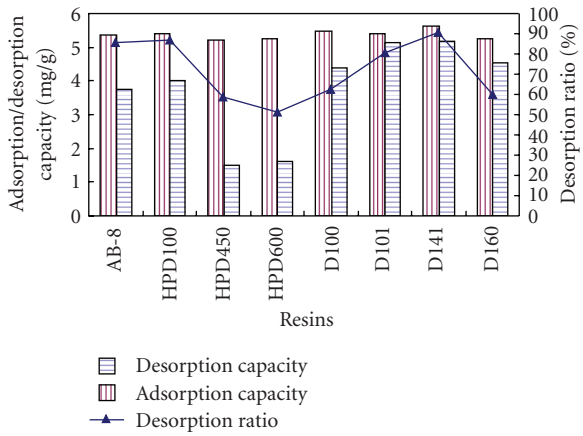

Figure 3: Adsorption capacity, desorption capacity, and desorption ratio of AG on different resins.

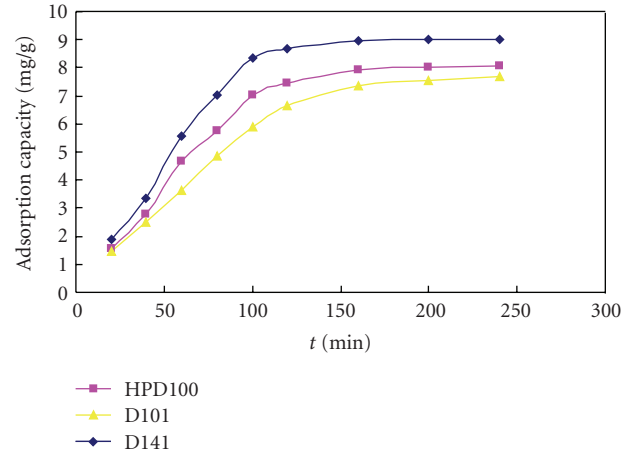

Figure 4: Adsorption kinetics curve for SG on HPD100, D101, and D141 resins.

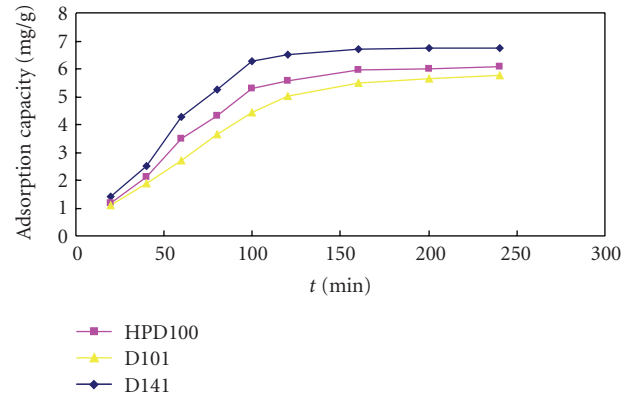

Figure 5: Adsorption kinetics curve for AG on HPD100, D101, and D141 resins.

The nonpolar resins HPD100 and D101, with specific surface areas and pore sizes suitable for adsorbing and desorbing SG and AG, also have better adsorption and desorption capabilities than other resins. Hence, HPD100, D101, and D141 resins were selected to further investigate their adsorption and desorption behavior towards SG and AG.

3.2. Adsorption Kinetics on HPD100, D101, and D141 Resins. Adsorption kinetics curves were obtained for SG and AG on HPD100, D101, and D141 resins. As shown in Figures 4 and 5, for the three resins studied, the adsorption capacities increased with the extension of adsorption time. At the beginning, the adsorption capacities increased rapidly; after 120 minutes they increased slowly and reached equilibrium at about 150 minutes for D141, D101, and HPD100 resins. The adsorption capacity of D141 towards SG was the highest at any time. In this study, the adsorption kinetics for AG showed similar tendency with SG. Hence, D141 resin was selected as the most suitable resin for the preparative separation of SG and was used in the further test.

3.3. Effect of Initial Solution pH. The pH value plays an important role in affecting the ionization of solutes, thus affecting their adsorption affinity between the solutes and solutions. The initial solution pH was adjusted to 3.0 ~ 12.0, respectively. Summarizing our data on the adsorption of the two flavone glucuronides from *E. multiradiatus*, we can conclude that the optimized conditions, which maximize the flavonol adsorptive capacity, include the use of the resin D141 and a totally aqueous solution, whatever its pH value, at least between 3.0 and 5.0.

3.4. Adsorption Isotherms on D141 Resin. Equilibrium adsorption isotherms were considered as important physicochemical aspects for the evaluation of the adsorption process. Langmuir and Freundlich equations are used to reveal the linearity fitting and to describe how solutes interact with the resins. Application of the Langmuir equation assumes monomolecular layer adsorption with a homogeneous distribution of adsorption energies and without mutual interaction between adsorbed molecules. Freundlich equation is used to describe the adsorption behavior of monomolecular

layer as well as that of the multimolecular layer. The model assumes a heterogeneous distribution among the adsorption sites at different energies.

Equilibrium adsorption isotherms were investigated with different temperatures of 25 °C, 30 °C, and 35 °C (Figures 6 and 7). The initial concentrations (C_0) of SG in the solutions were 1.18 mg/mL, 0.944 mg/mL, 0.708 mg/mL, 0.590 mg/mL, 0.354 mg/mL, and 0.118 mg/mL, respectively. The concentrations (C_0) of AG in the corresponding solutions were 0.81 mg/mL, 0.648 mg/mL, 0.486 mg/mL, 0.405 mg/mL, 0.243 mg/mL, and 0.081 mg/mL, respectively. The adsorption capacities increased with the increasing of the initial concentrations and reached the saturation plateau when the initial concentrations were 0.944 mg/mL and 0.648 mg/mL.

The experimental data were fitted to the Langmuir equation (4):

$$\frac{C_e}{q_e} = \frac{C_e}{q_o} + \frac{1}{Kq_o}, \tag{4}$$

where K is the adsorption equilibrium constant, and q_o is the empirical constant. The Langmuir equation was converted to the linearized form with C_e and C_e/q_e as independent variable, the experimental data were statistical analyzed, and R^2 were obtained.

The experimental data were also fitted to the Freundlich equation (5):

$$q_e = KC_e^{1/n}, \tag{5}$$

where K is the Freundlich constant that is an indicator of adsorption capacity, and $1/n$ value is obtained from the slope in linear regression result and an empirical constant related to indicate adsorptive energy or intensity. A linear equation is described as (6). A logarithmic plot linearizes the equation, enabling the exponent $1/n$ and the constant K to be determined:

$$\log q_e = \log K + \left(\frac{1}{n}\right) \log C_e. \tag{6}$$

The $1/n$ and K values can be obtained from the intercept and slope, respectively, and the linear regression line can also be generated from a plot of log q_e versus log C_e. The Langmuir and Freundlich parameters were summarized in Table 3. From Table 3 we can see that the correlation coefficients of both Langmuir and Freundlich equations were rather high.

In general, in the Freundlich equation (6), the adsorption can take place easily when the $1/n$ value is between 0.1 and 0.5, and it is not easy to generate if $1/n$ value is between 0.5 and 1; however, it is very difficult to occur if $1/n$ value exceeds 1 [13]. In the results, the $1/n$ values were all between 0.1 and 0.5, which suggested that D141 resin was favorable for the adsorption and separation of SG and AG from *E. multiradiatus*.

It can also be seen from Figures 6 and 7, within the range of temperatures investigated, at the same initial concentration, the adsorption capacities decreased with the increasing temperature; the adsorptive speed was slower than desorptive speed for both SG and AG, which indicated that the adsorption was a thermopositive process. Therefore, 25 °C was used in the following tests.

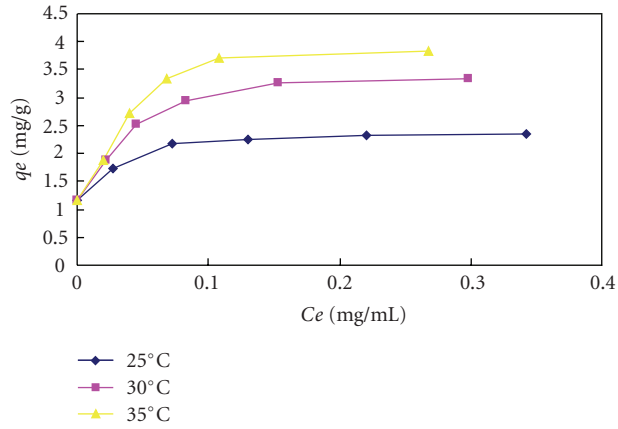

Figure 6: Adsorption isotherms for SG on D141 resin at 25 °C, 30 °C, and 35 °C .

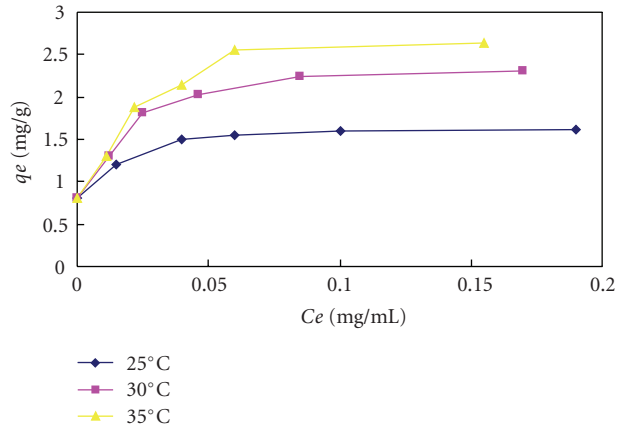

Figure 7: Adsorption isotherms for AG on D141 resin at 25 °C, 30 °C, and 35 °C.

3.5. Static Desorption on D141 Resin. For low cost and safety, ethanol-water was often chosen as desorption solution. Different concentrations of ethanol solutions, from 25% to 95% (v/v), were used to perform desorption test after adsorption equilibrium. As can be seen from Figure 8, at the beginning, the desorption ratios of both SG and AG increase accordingly with increasing of ethanol concentration. The maximum desorption ratios were found to be 88.7% and 90.2%, respectively, at a concentration of 55% ethanol. However, when the ethanol concentration is over 55%, the purity of the two constituents slightly decreased with increasing of ethanol concentration because more impurities with less polarity were desorbed at higher ethanol concentrations. Therefore, ethanol-water (55%, v/v) solution was considered as the appropriate desorption solution and was performed in the dynamic desorption process.

Table 3: Langmuir and Freundlich parameters of SG and AG on D141 resin at the temperature of 25 °C, 30 °C, and 35 °C.

	Temperature (°C)	Langmuir equation	R^2	Freundlich equation	R^2
SG	25	$C_e/q_e = 0.4201\,C_e + 0.0024$	0.9991	$q_e = 0.7252C_e^{0.2438}$	0.9721
	30	$C_e/q_e = 0.2883\,C_e + 0.0033$	0.9956	$q_e = 0.7742C_e^{0.2693}$	0.9683
	35	$C_e/q_e = 0.2498\,C_e + 0.0031$	0.9920	$q_e = 0.7923C_e^{0.2706}$	0.9637
AG	25	$C_e/q_e = 0.6085\,C_e + 0.0019$	0.9993	$q_e = 0.3161C_e^{0.1170}$	0.9716
	30	$C_e/q_e = 0.4193\,C_e + 0.0025$	0.9962	$q_e = 0.5609C_e^{0.2100}$	0.9668
	35	$C_e/q_e = 0.3622\,C_e + 0.0027$	0.9914	$q_e = 0.6858C_e^{0.2667}$	0.9650

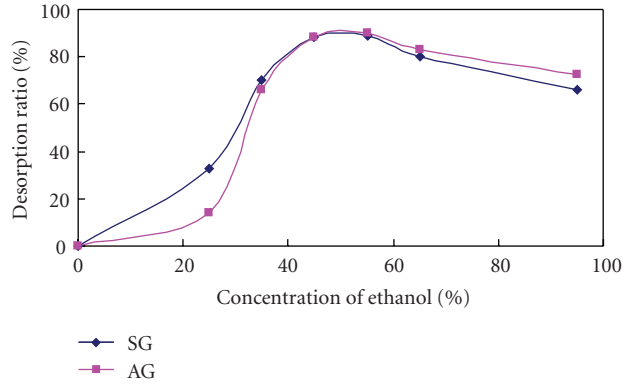

Figure 8: Effect of concentration of ethanol solution on the desorption ratio of SG and AG on D141 resins at 25 °C.

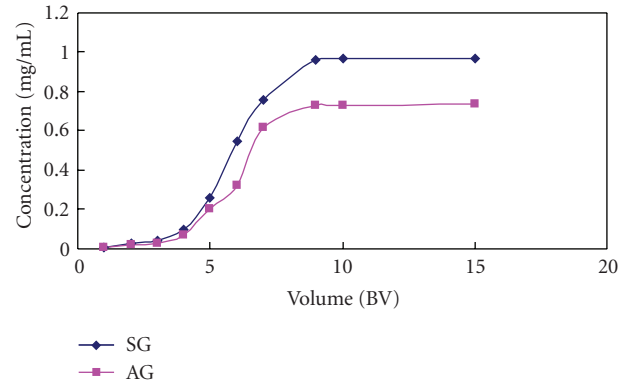

Figure 9: Dynamic leakage curves of SG, and AG on column packed with D141 resin.

3.6. Dynamic Leakage Curve on D141 Resin. The solute leakage from the column at breakthrough point was due to the resin in the column approached to be saturated. The breakthrough point was defined as 10% of the eluent to inlet solution concentration. Therefore, it is important to construct the leakage curve in order to calculate the quantity of resins, the processing volume of sample solution, and the proper sample flow rate. The dynamic leakage curves on D141 resin were obtained according to the volume of effluent liquid and the tested constituents' concentration. As shown in Figure 9, under this condition, the processing volume of sample solution on D141 resin was approximate 80 mL (4 BV) and the flow rate was 1.5 BV/h.

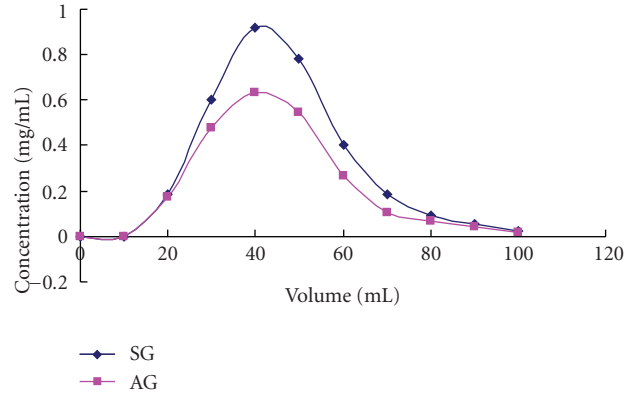

Figure 10: Dynamic desorption curves of SG, and AG on column packed with D141 resin.

3.7. Dynamic Desorption Curve on D141 Resin. According to the results of breakthrough volume determined above, the 80 mL sample solution was fed on the column packed with 5.0 g (dry weight) D141 resin. After adsoption equilibrium, the resin was firstly flushed with 80 mL of distilled water for removing the high polar components in the crude extraction of *E. multiradiatus*, such as polysaccharides and amino acids. And then the adsorbent was eluted with 55% ethanol aqueous. The dynamic desorption curves on D141 resin were obtained based on the volume of effluent and the concentration of solute therein. The flow rate in this test was 1.5 BV/h. As can be seen in Figure 10, a desorption solution of 100 mL (5 BV) could completely desorbed SG and AG from D141 resin. The desorption solution was analyzed by HPLC and then dried under vacuum. The dried product was weighed and the contents of SG and AG were calculated.

The dynamic desorption tests were repeated for 3 times under optimal parameters, and the RSD for recovery yield was calculated for both SG and AG. The chromatograms of the test samples before and after treatment with D141 resin were shown in Figure 11. By comparison, it can be found that some impurities were removed and the relative peak area of SG and AG increased obviously after the separation on D141 resin. After treatment with D141 resin, the content of SG and AG increased from 2.14% to 24.63% and from 1.34% to 18.42%, respectively, which were 11.52-fold and 13.75-fold, respectively, and the recoveries of them were 82.5% and

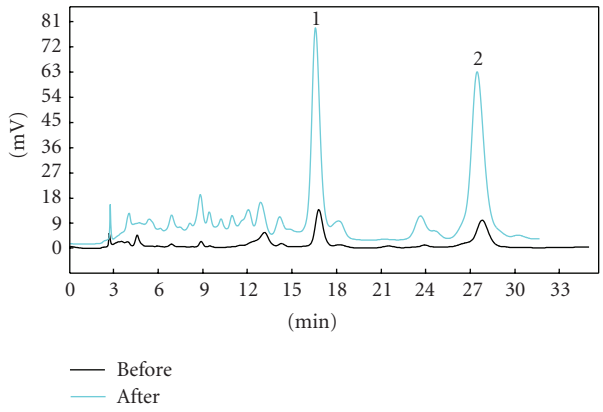

FIGURE 11: Chromatograms of sample solution before and after separation on a column packed with D141 resin. (1) Scutellarein-7-*O*-*β*-glucuronide; (2) Apigenin-7-*O*-*β*-glucuronide.

85.4%, respectively. And the RSD for recovery yield was 2.4 and 1.7%, respectively.

The optimum parameters for the preparative separation of SG and AG on D141 resin were confirmed as follows: for adsorption: sample solution SG and AG concentration 0.944 mg/mL and 0.648 mg/mL, respectively; pH4; processing volume 4 BV; flow rate 1.5 BV/h; temperature 25 °C; for desorption: elution solvent ethanol-water (55 : 45, v/v) solution 5 BV; flow rate 1.5 BV/h.

4. Conclusions

In this study, the adsorption and separation characteristics of SG and AG from *E. multiradiatus* extracts were evaluated on eight widely used macroporous resins. Among the eight resins investigated, D141 resin shows the best enrichment and purification efficiency. Some important parameters in the separation process, such as concentration and volume of feeding sample and concentration and volume of eluent, were optimized for most effective enrichment and preparative separation. Using D141 resin at optimal conditions, the content of SG and AG in the product was increased 11.52-fold and 14.75-fold, respectively. Gao prepared SG from *Erigeron breviscapus* (vant.) Hand. Mazz. by HPD800 macroporous resins [18]. The result is similar with us. However, both SG and AG were separated and enriched simultaneously in our experiment. This adsorption method is superior because of its procedural simplicity, lower cost, and high efficiency, and it may provide scientific references for the large-scale SG and AG production. The achievement of separation of SG and AG from *E. multiradiatus* will help for their pharmacological research and group separation from *Erigeron* genus and other herbs.

Acknowledgments

The authors thank the youth key science foundation by the Southwest University for Nationalities (Grant no. 26701601), the Bureau of Science and Technology of Sichuan Province for supporting this applied fundamental study (Grant no. 2006Z08–081).

References

[1] Z. Zhang, P. Luo, J. Li, et al., "Comparison of the anti-inflammatory activities of three medicinal plants known as "meiduoluomi" in Tibetan folk medicine," *Yakugaku Zasshi*, vol. 128, no. 5, pp. 805–810, 2008.

[2] Z. Zhang, W. Sun, P. Luo, L. Wu, L. Ye, and H. Zhang, "Simultaneous determination of five main active constituents of *Erigeron multiradiatus* by HPLC-DAD-MS," *Journal of Pharmaceutical and Biomedical Analysis*, vol. 48, no. 3, pp. 980–985, 2008.

[3] B.-H. Zhu, Y.-Y. Guan, H. He, and M.-J. Lin, "Erigeron breviscapus prevents defective endothelium-dependent relaxation in diabetic rat aorta," *Life Sciences*, vol. 65, no. 15, pp. 1553–1559, 1999.

[4] S. Nagashima, M. Hirotani, and T. Yoshikawa, "Purification and characterization of UDP-glucuronate: baicalein 7-O-glucuronosyltransferase from *Scutellaria baicalensis* Georgi. cell suspension cultures," *Phytochemistry*, vol. 53, no. 5, pp. 533–538, 2000.

[5] J. Qu, Y. Wang, and G. Luo, "Determination of scutellarin in *Erigeron breviscapus* extract by liquid chromatography-tandem mass spectrometry," *Journal of Chromatography A*, vol. 919, no. 2, pp. 437–441, 2001.

[6] H. Hong and G.-Q. Liu, "Protection against hydrogen peroxide-induced cytotoxicity in PC12 cells by scutellarin," *Life Sciences*, vol. 74, no. 24, pp. 2959–2973, 2004.

[7] X. Ma, L. Wu, Y. Ito, and W. Tian, "Application of preparative high-speed counter-current chromatography for separation of methyl gallate from *Acer truncatum* Bunge," *Journal of Chromatography A*, vol. 1076, no. 1-2, pp. 212–215, 2005.

[8] J. Peng, G. Fan, L. Qu, X. Zhou, and Y. Wu, "Application of preparative high-speed counter-current chromatography for isolation and separation of schizandrin and gomisin A from *Schisandra chinensis*," *Journal of Chromatography A*, vol. 1082, no. 2, pp. 203–207, 2005.

[9] J. Chang and R. Case, "Phenolic glycosides and ionone glycoside from the stem of *Sargentodoxa cuneata*," *Phytochemistry*, vol. 66, no. 23, pp. 2752–2758, 2005.

[10] E. Tanaka, C. Tanaka, N. Mori, Y. Kuwahara, and M. Tsuda, "Phenylpropanoid amides of serotonin accumulate in witches' broom diseased bamboo," *Phytochemistry*, vol. 64, no. 5, pp. 965–969, 2003.

[11] L. Dunn, M. Abouelezz, L. Cummings, et al., "Characterization of synthetic macroporous ion-exchange resins in low-pressure cartridges and columns: evaluation of the performance of Macro-Prep 50 S resin in the purification of anti-Klenow antibodies from goat serum," *Journal of Chromatography*, vol. 548, no. 1-2, pp. 165–178, 1991.

[12] Y. Fu, Y. Zu, W. Liu, et al., "Optimization of luteolin separation from pigeonpea [*Cajanus cajan* (L.) Millsp.] leaves by macroporous resins," *Journal of Chromatography A*, vol. 1137, no. 2, pp. 145–152, 2006.

[13] B. Fu, J. Liu, H. Li, L. Li, F. S. C. Lee, and X. Wang, "The application of macroporous resins in the separation of licorice flavonoids and glycyrrhizic acid," *Journal of Chromatography A*, vol. 1089, no. 1-2, pp. 18–24, 2005.

[14] B. Zhang, R. Yang, Y. Zhao, and C.-Z. Liu, "Separation of chlorogenic acid from honeysuckle crude extracts by

macroporous resins," *Journal of Chromatography B*, vol. 867, no. 2, pp. 253–258, 2008.

[15] G. Jia and X. Lu, "Enrichment and purification of madecassoside and asiaticoside from *Centella asiatica* extracts with macroporous resins," *Journal of Chromatography A*, vol. 1193, no. 1-2, pp. 136–141, 2008.

[16] X. Liu, G. Xiao, W. Chen, Y. Xu, and J. Wu, "Quantification and purification of mulberry anthocyanins with macroporous resins," *Journal of Biomedicine and Biotechnology*, vol. 2004, no. 5, pp. 326–331, 2004.

[17] H. Li, J.-H. Lee, and J.-M. Ha, "Effective purification of ginsenosides from cultured wild ginseng roots, red ginseng, and white ginseng with macroporous resins," *Journal of Microbiology and Biotechnology*, vol. 18, no. 11, pp. 1789–1791, 2008.

[18] M. Gao, W. Huang, and C.-Z. Liu, "Separation of scutellarin from crude extracts of *Erigeron breviscapus* (vant.) Hand. Mazz. by macroporous resins," *Journal of Chromatography B*, vol. 858, no. 1-2, pp. 22–26, 2007.